Photoelectrical Properties and Energetical Structure of Thin Films of Indandione Derivatives

Maira INDRIKOVA [1], Janis LATVELS [1][*], Inta MUZIKANTE [1], Baiba TUROVSKA [2]

[1] *Laboratory of Organic Materials, Institute of Solid State Physics, University of Latvia,*
Kengaraga St. 8, LV-1063 Riga, Latvia
[2] *Latvian Institute of Organic Synthesis, Aizkraukles St. 21, LV-1006 Riga, Latvia*

A sandwich type structure of two dimetilaminobenziliden-1,3-indandione (DMABI) derivatives placed between metal electrodes was made to investigate the photoelectrical properties of these derivatives. DMABI is an organic isolator with a wide energy gap and high quantum efficiency of the photogeneration, DMABI derivatives have received also considerable attention because of its large dipole moment and optical nonlinearities. Besides, since it is a photosensitive material, its use in solar systems is very promising. The energy gap of each material and combined system was observed from the spectral dependence of the quantum efficiency of the photoconductivity and results are compared with results of oxidation and reduction potential of the materials. The values showed a good correlation between experimental data of the photoconductivity and voltamperometry and calculated data of the HOMO and LUMO levels of the molecules.

Keywords: quantum efficiency of the photoconductivity, sandwich type structure, energetical structure, photogeneration, indandione.

1. INTRODUCTION

Recently, there has been a great interest in organic solar cells. Such solar cells are an innovative and at the same time a perspective field [1–4]. Organic materials help to reduce the costs of solar cells and simplify the production process. However, further investigations are necessary to improve the efficiency and the lifetime of organic solar cells. To achieve higher efficiency, it is important that a molecule absorbs light in a spectral region close to the Sun spectrum. Nevertheless, fundamental part to design effective solar cells is knowledge of energetic characteristics of a material. Parameters such as ionization potential I_C, electronaffinity A_C and energy gap E_G directly affects such important electronic processes as charge carrier generation and transport [5–7]. These parameters are useful to create the energy diagram both of a material and structures electrode/organic layer/electrode (M/OL/M). In order to have complete energetical diagram of thin film structure consisting of two electrodes the values of work function of electrodes are necessary.

In case of organic crystals charge carriers do not emerge as "bare"quasi-free electrons and holes but as a polaron type quasi-particle, dressed "in electronic and vibronic polarization clouds" [7, 8]. After excitation of molecules the ion pair is formed. Electronically relaxed charges may also be formed far enough from each other in order to neglect ion pair energy. This process corresponds to optical band gap E_G^{Opt} [7, 9]. The value E_G^{Opt} is usually measured as the energy of the long wavelength edge of an exciton absorption band, where the normalized absorption and fluorescence spectra intersect [9] or from electromodulated absorption spectra [8]. When both vibrationally and electronically relaxed states are considered as adiabatic energy gap E_G^{Ad}. To determine the adiabatic energy gap E_G^{Ad}, one must measure the charge carrier energies after their vibronic relaxation to the molecular polaron states. Besides the values of E_G^{Ad} and E_G^{Opt}, the value of transport band E_t is applied as a difference between the values of the highest occupied molecular level (HOMO) and the lowest unoccupied molecular level (LUMO), which are measured by ultraviolet photoelectron spectroscopy (UPS) and inverse photoelectron spectroscopy (IPES) of the material [10]. There are several methods to determine the value of the E_G^{Ad}. In nineties one of the most popular method to obtain the energy gap in low molecular organic thin films and crystals was photoelectrical method [5, 8]. It has been shown that in anthracene-type crystals the spectral dependence of quantum efficiency of intrinsic photoconductivity $\beta(h\nu)$ is determined by the efficiency of the thermal dissociation of the ion pairs formed as an intermediate stage of the photogeneration process, which may be described by the Onsager mechanism. The quantum efficiency of intrinsic photoconductivity $\beta(h\nu)$ in the near threshold region can be approximated by

$$\beta(h\nu) = A(h\nu - E_{th})^n, \tag{1}$$

where $n \approx 5/2$ and E_{th} is the threshold of intrinsic conductivity and A is coefficient [5, 8].

The value of the photoconductivity threshold E_{th} allows to obtain the value of adiabatic energy gap E_G^{Ad} [5, 8], i. e.,

$$E_G^{Ad} = E_{th} + \Delta E, \tag{2}$$

where ΔE is effective relaxation energy of the ion pair state.

It is a complex problem to obtain spectral curves of intrinsic photoconductivity. The experiments have to be

[*]Corresponding author. Tel.: + 371-67260787; fax.: + 371-67132778
E-mail address: *janis.latvels@gmail.com* (J. Latvels)

done under completely blocked injection of the charge carriers from the electrodes. However, in many cases extrinsic photogeneration and injection of charge carrier from the electrodes should be taken into account. In accordance with the concept of the photogeneration mechanisms one may assume that the charge carriers, which are involved in stationary photoconductivity are already completely relaxed, and the threshold value E_{th} reflects the value of the adiabatic energy gap. However, as E_{th} according to definition is situated at the very threshold of the $\beta(h\nu)$ curves we may assume that the value of E_{th} is slightly lower than expected adiabatic energy gap. It is shown in the polyacene crystals [8] the following correlation $E_{th} < E_G^{Ad} < E_G^{Opt}$ is available.

On the other hand, the adiabatic energetic gap E_G^{Ad} could be estimated from the electrochemical redox potentials obtained by cyclic voltammetry (CV) [9, 11–13]. The first standard reduction potential (E_{red}^0) of the compound measured in the solution and gas phase electron affinity (A_C) are linearly related between each other. Similarly the first standard oxidation potentials (E_{ox}^0) correlated linearly with the ionization potentials (I_C). For the organic molecules with the large delocalized π electron systems where the gain or loss of an electron introduces small disturbances the slopes of both correlations are close to the unity.

In the first approximation the optical band gap E_G^{Opt} corresponds to the difference between ionization potential I_C and the electron affinity A_C of the molecule. In the literature [9] it has been confirmed that the difference between the oxidation and reduction potentials $\Delta E_{redox}^0 = E_{ox}^0 - E_{red}^0$ closely corresponds to the optical band gap E_G^{Opt}.

The aim of the research is to report on the results obtained by investigating two derivatives of dimetilaminobenzylidene-1,3-indandione (DMABI), where in indandione part of the molecules one carbon is substituted by nitrogen atom (4N-DMABI-dPh) or added tert-butyl group (tBu-DMABI-dPh) (Figure 1). The research was done in collaboration with chemists of Riga Technical University who synthesized the derivatives necessary for the investigation [14].
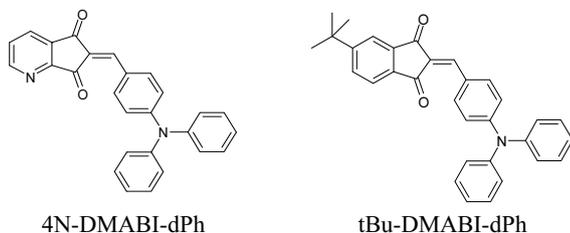
Fig. 1. Chemical structure of DMABI derivatives under study: 4N-DMABI-dPh and tBu-DMABI-dPh

According to the RHF *ab initio* calculations with basis set 6-31G** by Gaussian G09W software package, the values of the HOMO and the LUMO levels of both derivatives are estimated. The calculated HOMO and LUMO values of the 4N-DMABI-dPh molecule are –7.25 eV and 1.39 eV and of the tBu-DMABI-dPh molecule –7.34 eV and 1.04 eV, respectively. The HOMO level characterizes the ionization potential I_G of the molecule. We see that calculated values of the ionization potential are in the range 7.2 eV – 7.3 eV, which is typical for electron donors used for strong charge transfer complexes [15]. The shift of HOMO and LUMO levels may be formed as an energy barrier between both molecular materials and heterojunction in double layer structure between 4N-DMABI and tBu-DMABI-dPh is prospective.

In this work, photoelectrical properties of DMABI derivatives are investigated, both for single layer and double layer samples. Our studies are based on the formation of the M/OL/M structures consisting of one layer of 4N-DMABI-dPh or tBu-DMABI-dPh molecules and double-layer structure consisting of the heterojunction between them. Sample M/OL/M was made as organic thin film, which was sandwiched between two metal electrodes.

The quantum efficiency of photoconductivity $\beta(h\nu)$ was measured for one layer and double-layer organic thin films in dependence on the polarity of the illuminated electrode. The value of band gap E_G^{Ad} of each material M/OL/M system was estimated from the quantum efficiency of the intrinsic photoconductivity $\beta(h\nu)$ curves in the threshold spectral region. The E_{th} values were compared with $\Delta E_{redox}^0 = E_{ox}^0 - E_{red}^0$ results of electrochemical method.

2. EXPERIMENTAL

2.1. Samples preparation

The samples were fabricated in a typical sandwich type structure on the glass substrates. For the construction of single layer and double layer samples two organic compounds were used: 4N-DMABI-dPh and tBu-DMABI-dPh. The layers of the samples were made by vacuum deposition method. The depositions started by gold layer as the bottom electrode (average thickness was about 50 nm) Then, the organic layers were deposited at temperature 190 °C with average thickness ~250 nm. The Al electrodes were deposited on the top of the system with average thickness 50 nm. Overall, for the system up to four masks were used for the preparation, without breaking the vacuum ($\approx 10^{-6}$ mbar) between each stage. The active area of the sample was about 0.02 cm^2. The thicknesses of layers were measured using surface profiler "Veeco Dektak 150" and the absorption spectra were measured by spectrometer "Ocean Optics HR4000 UV-NIR".

2.2. Measurements of the cyclic voltammetry

Electrochemical properties of DMABI derivatives were studied by cyclic voltammetry (CV). The curves were recorded on the electrochemical system PARSAT 2273 using glassy carbon disk (Ø 0.5 cm) as a working electrode. Saturated calomel electrode (SCE) was served as a reference electrode and Pt wire – as an auxiliary electrode. (Fig.2)
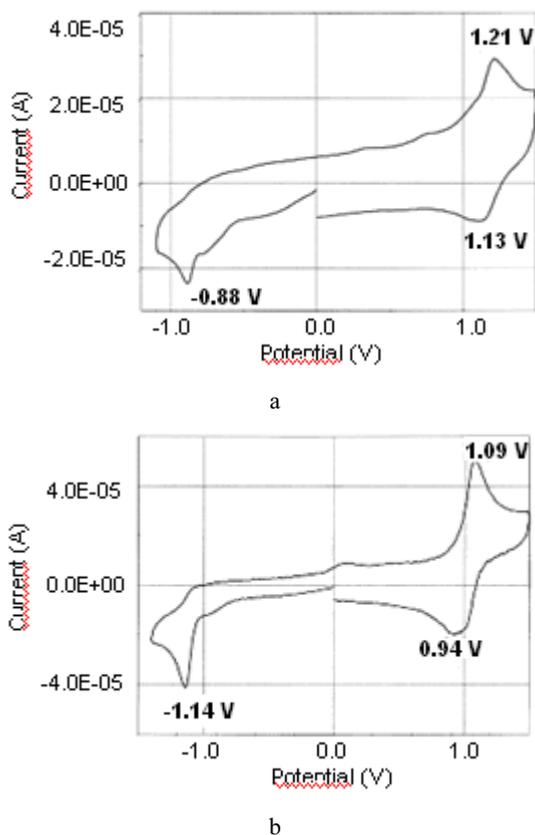
Electrochemical redox reactions were studied in deareated 0,1 M tetrabutyl-ammoniumtetrafluorophosphate (TBAPF$_6$) solution in acetonitrile.

2.3. Photoelectrical measurements

The electrical properties (current-voltage characteristics and spectral dependence of the photocurrent) of single layer devices (Au/4N-DMABI-dPh/Al and Au/tBu-DMABI-dPh/Al) and double layer device (Au/4N-DMABI-dPh/tBu-DMABI-dPh)) were measured in a vacuum cryostat, which was connected with *CDK250* turbomolecular pump systems. All measurements were performed in vacuum using an electrometer *KEITHLEY 6517B* with an incorporated DC voltage supply. As a light source Xenon lamp *TYP SVX 1450* with power supply was used. In front of the lamp Andover Corporation interference filters (from 360 nm – 700 nm, with the step 20 nm) were placed, after them the lens' system and shutter. The final was the optical wire, which was directed to the sample in the vacuum camera and had been irradiated through the small quartz glass window in the cryostat.

The samples were irradiated from the top Al electrode (Fig. 3, a) and from the bottom Au electrode (Fig. 3, b). All the measurements have been applied for both polarities.

The quantum efficiency of the photoconductivity $\beta(h\nu)$ was estimated according to the equation [5]:

$$\beta(h\nu,U) = \frac{j_{ph}(h\nu,U)}{e\,k(h\nu)\,I(h\nu)\,g(h\nu)} ,\qquad (3)$$
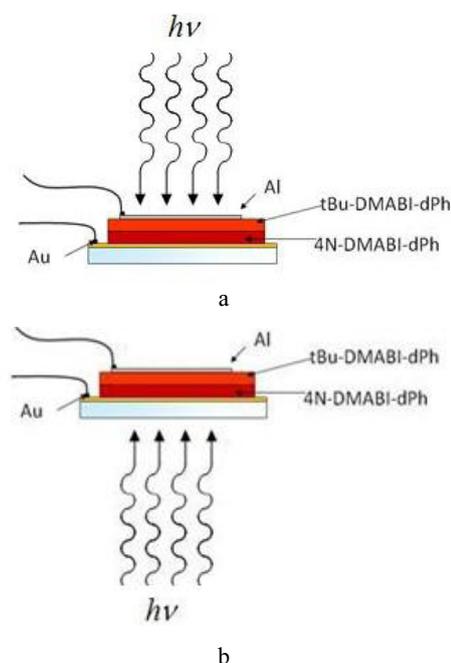
Fig. 3. Schemes of irradiation of the sample from the top Al electrode (a) and from the bottom Au electrode (b)

where j_{ph} is the density of photocurrent at a given photon energy $h\nu$ and applied voltage U, $I(h\nu)$ is the intensity of light (phot/cm^{2}s), $k(h\nu)$ is the transmission of semitransparent electrode, $g(h\nu)$ is the coefficient which characterizes the absorbed light in the organic layer:

$$g(h\nu)=\int_0^L [\exp(-\alpha(h\nu)x]dx =1-\exp(-\alpha(h\nu)L) ,\qquad (4)$$

where $\alpha(h\nu)$ is the absorption coefficient of the organic film and L is the thickness of the film.

3. RESULTS AND DISCUSSION

DMABI and it's derivatives are organic materials with high resistivity ρ up to $\rho \approx 10^{11}$ Ωcm. These compounds are practically isolators. DC current-voltage characteristics $I(U)$ were studied at the room temperature in the voltage region up to 60 V of one organic layer samples and up to 100 V of double organic layer samples (Fig. 4). As it is shown in the Fig. 4, a, b, the superlinear dependence of the dark current on voltage of single layer samples occurred. IU-characteristics demonstrate almost symmetry of current dependent on the conditions of injection of charge carriers from the bottom Au or the top Al electrode. In case of holes injection from the bottom Au electrode, the super-linear IU characteristics appeared at electric field values ($E \geq 4.5×10^5$ V/cm) in comparison with holes injection from the upper Al electrode ($E \geq 5×10^5$ V/cm). Consequently, the photoconductivity spectral dependence of single layer sample was measured at the voltage U = 10 V ($E \approx 4×10^5$ V/cm), where conditions of blocked injection of charge carriers from the electrodes may be fulfilled. In case of double layer structure the IU-characteristics (Fig. 4, c) are superlinear dependence whereas the asymmetry of current dependent on the conditions of injection of charge carriers from the bottom

Au or the top Al electrode were observed. The rectification effect found, when Au is positively biased.

4N-DMABI-dPh
Au+
Au−
a

tBu-DMABI-dPh
Au+
Au−
b

4N-DMABI-dPh/tBu-DMABI-dPh
Al+
Al−
c
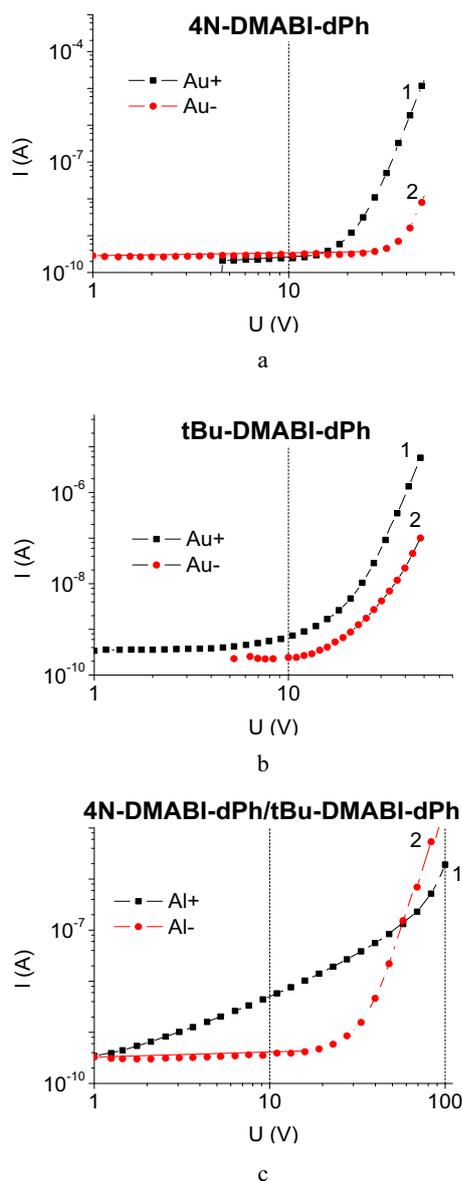
Fig. 4. Current voltage characteristics of Au/4N-DMABI-dPh/Al (a), Au/tBu-DMABI-dPh/Al (b) and Au/4N-DMABI/tBu-DMABI/Al (c) samples, measured at room temperature in darkness and vacuum with positive Au and positive Al electrodes

DMABI and its derivatives belong to the class of photosensitive molecular crystals. By irradiation with ultraviolet and visible light the current increases by several orders of magnitude [18]. When 4N-DMABI-dPh and tBu-DMABI-dPh single layer samples were irradiated the fast increase of the current up to one order of the magnitude was observed. As an example in the Fig. 5 the time dependence of current on irradiation of 4N-DMABI single layer sample is presented. When the light was switched off the process was reversible with almost the same response time.

The density of photocurrent j_{ph} at a given photon energy $h\nu$ was calculated as $j_{ph} = j_f - j_d$, where j_d is the current measured in the darkness, j_f is the current measured during irradiation.

4N-DMABI-dPh, U=10V, Au−
620nm
640nm
540nm
500nm
440nm
380nm
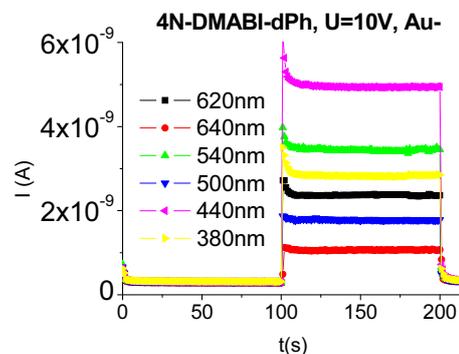
Fig. 5. Photocurrent kinetic of the Au/4N-DMABI/Al on irradiation via negative Au electrode at different wavelengths. Irradiation starts at 100 s and lasts 200 s

The spectral photoconductivity dependences were measured in the spectral range from $\lambda = 360$ nm to $\lambda = 700$ nm. The quantum efficiency of photoconductivity $\beta(h\nu)$ was obtained according to the equation (3). Typical dependences $\beta(h\nu)$ in the threshold region are shown in the Fig. 6a and 7a.

The spectral dependences of $\beta(h\nu)$ on irradiation through Au and Al electrodes of both polarities were compared. Fig. 6, a, shows that $\beta(h\nu)$ curves when sample is irradiated through negative Au and negative Al electrodes are similar with two maxima which correspond to long and short wavelengths sides of the absorption maximum of 4N-DMABI-dPh thin film. In case of irradiation through positive Au and positive Al electrodes only one maximum of $\beta(h\nu)$ was observed. Nevertheless, the maximal value of $\beta(h\nu)$ in all cases close to 1.5×10^{-4} el/phot was observed. The anti-correlation of $\beta(h\nu)$ and $\alpha(h\nu)$ curves means that the photogeneration process in thin film volume dominates over the processes in the interface between electrode and organic thin film. Increase of the value of $\beta(h\nu)$ at irradiation lower than 2.0 eV may be caused by optically induced release of charge

Table 1. The values of the oxidation E^0_{ox}, reduction E^0_{red} and redox E^0_{redox} potentials of DMABI, 4n-DMABI-dPh and tBu-DMABI-dPh in TBAPF$_6$ solution, threshold value of photoconductivity of E_{th} of their thin films

Molecule	Oxidation		Reduction		ΔE (eV)	E_{th} (eV)	|HOMO-LUMO|
	E^a_{ox}(eV)	E^c_{ox}(eV)	E^o_{ox}(eV)	E^c_{red}(eV)			
4N-DMABI-dPh	1.21	1.13	1.17	−0.88	2.05	1.80 ±0.05	8.38
tBu-DMABI-dPh	1.09	0.94	1.02	−1.14	2.16	1.90 ±0.05	8.64
DMABI	0.98	0.89	0.94	−1.27	2.21	1.95 ±0.02 [10]	8.45
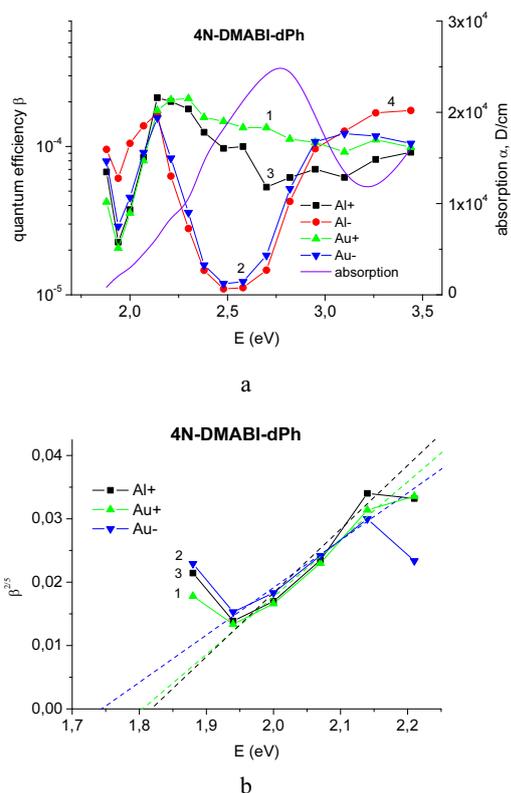
Fig. 6. (a) Spectral dependences of the photocurrent of Au/4N-DMABI/Al. Irradiation of the sample is carried out via positive Au electrode (1), negative Au electrode (2), positive Al electrode (3) and negative Al electrode (4) at $U = 10$ V. The absorption spectrum of 4N-DMABI thin film is presented. (b) Approximation of threshold of the intrinsic photoconductivity E_{th} according to equation (1)

Fig. 7. (a) Spectral dependences of the photocurrent of Au/tBu-DMABI/Al. Irradiation of the sample is carried out via positive Au electrode (1), negative Au electrode (2), positive Al electrode (3) and negative Al electrode (4) at U=10V. The absorption spectrum of tBu-DMABI thin film is presented by solid line (b) Approximation of threshold of the intrinsic photoconductivity E_{th} according to the equation (1)

carriers from traps. The value of the band gap energy was estimated as the threshold value $E_{th} = 1.80$ eV ± 0.05 eV according to the expression (1) (Fig. 6, b).

In aprotic acetonitrile electrochemical oxidation of amine moiety in DMABI and its derivatives proceeds in one quasi-reversible step (Fig. 2). Calculated standard oxidation potentials (E_{ox}^0) of the compounds are given in the Table 1.

Whereas electrochemical reduction of indandione moiety of DMABI and its derivatives proceeds in one irreversible step at the potential scan rate 100 mV/sec. However, an irreversible peak potential may correspond to within 100 mV of the reversible reduction potential [16] if the species generated by reversible electron transfer process is consumed by rapid chemical follow-up reaction, like protonation [17].

Fig. 7, a, shows that $\beta(h\nu)$ curves in all four cases are similar with two maxima which corresponds to long and short wavelengths sides of the absorption maximum of tBu-DMABI-dPh thin film. The maximal value of $\beta(h\nu)$ in all cases close to 4×10^{-4} el/phot was observed. The maximal values of $\beta(h\nu)$ of 4N-DMABI-dPh and tBu-DMABI-dPh films are lower by two orders of magnitude than of the DMABI thin film [18]. The anti-correlation of $\beta(h\nu)$ and $\alpha(h\nu)$ curves meaning is the same as in the situation for 4N-DMABI-dPh. The value of the band gap

energy was estimated as the threshold value $E_{th} = 1.90$ eV ± 0.05 eV according to the expression (1) (Fig. 7, b).

The results of quantum efficiency of photoconductivity and cyclic voltamperometry are presented in the Table 1 (for comparison the energetical values of DMABI thin films are presented).

The threshold energy of E_{th} is 1.95 eV ± 0.02 eV [18]. The value of optical band gap E_G^{Opt} as the energy of the long wavelength edge of an exciton absorption band, where the normalized absorption and fluorescence spectra intersect of the DMABI films is estimated to be 2.15 eV ± 0.02 eV [19]. As it is presented in the Table 1, the correlation between the values of E_{th}, and ΔE_{redox} is observed.

The spectral dependencies of photoconductivity of double layer Au/4N-DMABI-dPh/tBu-DMABI-dPh/Al device were measured at voltage $U = 10$ V.

As follows from the Fig. 4, the IU-curves at the voltage 10 V and positive Au polarities showed blocking properties similar to single layer devices. On the other side, when positive Al electrode was applied, in the current dependence on voltage is linear at up to $U = 11$ V, i. e., $I \sim U$, typical for Ohmic-type conductivity. According to the model of the space charge limited conductivity the injection of holes from Al electrode to tBu-DMABI-dPh is
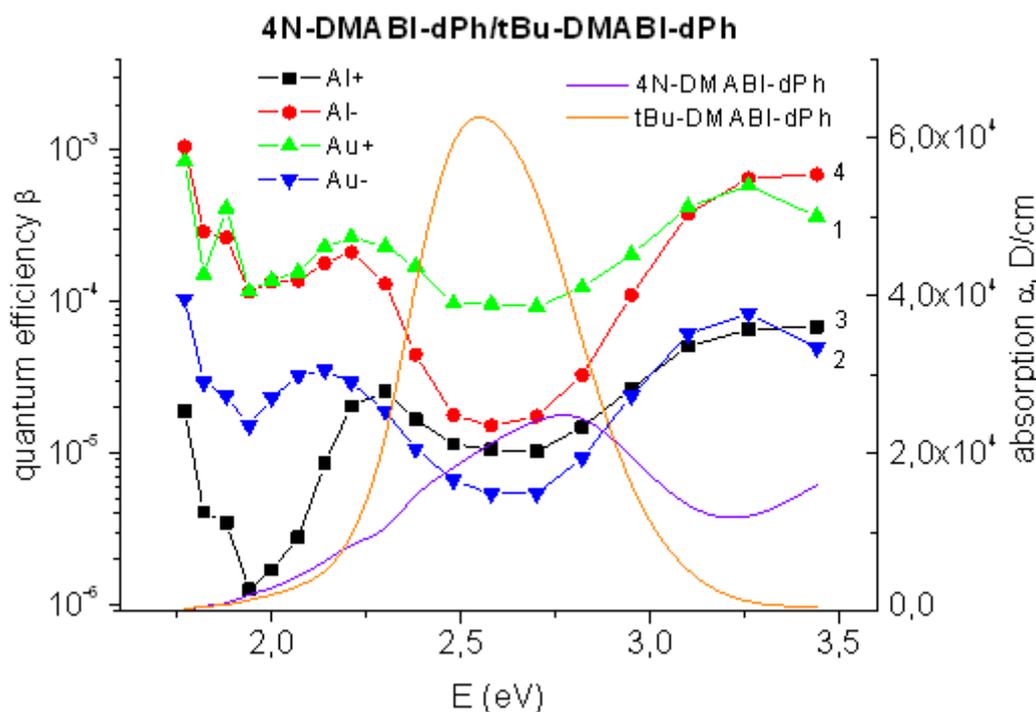
Fig. 8. Spectral dependences of the photocurrent of Au/4N-DMABI/tBu-DMABI/Al. Irradiation of the sample is carried out via positive Au electrode (1), negative Au electrode (2), positive Al electrode (3) and negative Al electrode (4) at $U = 10$ V. The absorption spectra of tBu-DMABI thin film and 4N-DMABI thin film are presented by solid line

possible. The spectral dependence of quantum efficiency $\beta(h\nu)$ is presented in the Fig. 8.

In case of double layer device in the equation (3) the intensity of the absorbed light is modified. The total absorbed light:

$$I = I_0[1 - \exp(\alpha_1 L)] + I_0 \exp(-(\alpha_1 L_1)\,[1 - \exp(\alpha_2 L_2)]\,. \quad (5)$$

When the Au electrode is positive the $\beta(h\nu)$ curves are similar to the spectra of $\beta(h\nu)$ of single layer 4N-DMABI-dPh device and independent on direction of irradiation and the $\beta(h\nu)$ values are close to one of single layer 4N-DMABI-dPh (Fig. 6). The same was observed when Al electrode was positive and character of the $\beta(h\nu)$ and values corresponds to the results of single-layer devices of tBu-DMABI-dPh (Fig 7). So, we may conclude that $\beta(h\nu)$ values character is mainly determined by polarity of the electrodes but direction of irradiation. N. Karl and co-authors [3] have investigated the photovoltaic short circuit current spectra of the double layer structure of the H_2-phthalocyanine and perylene derivative PTCDA or naphthalene derivative NTCDA. They have shown that the photocurrent of these double layer structures depends on the order of the organic layers and polarity of the electrode but not on the electrode that is illuminated.

4. CONCLUSIONS

The value of quantum efficiency $\beta(h\nu)$ for the single layer thin films – 4N-DMABI-dPh is about 1×10^{-5} el/phot and for the tBu-DMABI-dPh films approximately 1×10^{-4} el/phot in the spectral range from 1.9 eV till 2.3 eV. In comparison with DMABI thin films, the values are lower by two orders of magnitude.

The quantum efficiency of photoconductivity $\beta(h\nu)$ of double layer devices mainly depends on the polarity of electrodes, but on the direction of irradiation. In case of positive Au electrode dominates photoelectrical properties of the 4N-DMABI-dPh layer which is deposited on Au electrode. Whereas, in case of positive Al electrode dominates properties of the tBu-DMABI-dPh layer.

The photoconductivity threshold energy for 4N-DMABI-dPh films is $E_{th} = 1.80$ eV ±0.05 eV and for tBu-DMABI-dPh films is $E_{th} = 1.90$ eV ±0.05 eV.

The threshold values are close to the redox potential ΔE_{redox} values of 4N-DMABI-dPh and tBu-DMABI-dPh molecules which are $\Delta E_{redox} = 2.05$ eV and $\Delta E_{redox} = 2.16$ eV respectively. Besides, the difference of calculated HOMO and LOMO levels of the molecules also correlates with threshold energies.

REFERENCES

1. Organic Photovoltaics: Mechanisms, Materials, and Devices. Eds. **S.-S. Sun**, **N. S. Sariciftci**. CRC Press, Taylor and Francis Group, 2005.

2. Organic photovoltaics. Concepts and Realization. Eds. **J. C. Brabec, V. Dyakonov, J. Parisi, N. S. Sariciftci.** Springer-Verlag, Berlin, Heidelberg, 2003

3. **Karl, N., Bauer, A., Holzzäpfel, H., Marktanner, J., Möbus, M., Stölzle, F.,** Efficient Organic Photovolataic

Cells *Molecular Crystals and Liquid Crystals* 252 1994: pp. 243 – 258.

4. Polymer Photovoltaics. A Practical Approach. Ed. **F. C. Krebs**. SPIE Press, Bellingham, Washington, 2008.

5. **Silinsh, E. A.** Organic Molecular Crystals. Their Electronic States. Springer Verlag, Berlin, Heidelberg, NY, 1980.

6. **Pope, M., Swenberg, C. E.** Electronic Processes in Organic Crystals and Polymers. Oxford University Press, New York, Oxford, 1999: 1328 p.

7. **Silinsh, E. A., Capek, V.** Organic Molecular Crystals. Interaction, Localization and Transport Phenomena. AIP Press, New York, 1994.

8. **Silinsh, E. A., Bouvet, M., Simon, J.** Determination of Energy Gap Values in Molecular Crystals *Molecular Materials* 5 1995: pp. 1 – 24.

9. **Djurovich, P. I., Mayo, E. I., Forest, S. R., Thompson, M. E.** Measurement of the Lowest Unoccupied Molecular Orbital Energies of Molecular Organic Semiconductors *Organic Electronics* 10 2009: pp. 515 – 520.

10. Conjugated Polymer and Molecular Interfaces. Science and Technology for Photonic and Optoelectronic Applications. Eds. **W. R Salaneck, K. Seki, A. Kahn, J.-J. Pireaux**. Marcel Dekker Inc., New York, Basel, 2002.

11. **Gutman, F., Lyons, L.** Organic Semiconductors. J.Wiley Inc., New York, 1967.

12. **Bouvet, M., Silinsh, E. A., Simon, J.** Determination of Energy Gap Values in Molecular Crystals. II. Intrinsic Dark Conductivity and Electrochemical Methods *Molecular Materials* 5 1995: pp. 255 – 277.

13. **Micaroni, L., Nart, F. C., Hümmelgen, I. A.** Conside-Rations about the Chemical Estimation of the Ionization Potential of Conducting Polymers *Journal of Solid State Electrochemistry* 7 2002: pp. 55 – 59.

14. **Kampars, V., Pastors, P.** Determination of Solvents Characteristics by Comparison the 4-AZA-2-(4'-Dimethyl aminobenzylidene)-1,3-indanedione and 2-(4'-Dimethyl aminobenzylidene)-1,3-indanedione Solvatechromy *Scientific Proceedings of Riga Technical University. Material Science and Applied Chemistry* 18 2008: pp. 103 – 108.

15. **Neilands, O.** Problems in Search for Strong Organic Electron Donors and Electron Acceptors *Latvian Journal of Physics and Technical Sciences* 6 1981: pp. 63 – 77.

16. **Howell, O., Goncalves, J. M., Amatore, C., Klasinc, L., Wightman, R. M., Kochi, J. K.** Electron Transfer from Aromatic Hydrocarbons and Their pi-complexes with Metals *Journal of the American Chemical Society* 106 1984: pp. 3968 – 3976.

17. Structure and Tautomerism of β-dicarbonyl Compounds. Eds. **E. Gudriniece, S. Hiller, E. Grens, O. Neilands, J. Stradins**. Zinatne, Riga, 1977.

18. **Kaulach, I., Silinsh, E. A.** Spectral Dependence of Magnetic Field Effect on Photoconductivity of Dimethhyl-aminobenzylidene1,3-indandione *Latvian Journal of Physics and Technical Sciences* 3 1997: pp. 3 – 10.

19. **Juršėnas, S., Gulbinas, V., Gustavson, T., Mialocq, J.-C., Valkūnas, L.** Femtosecond Fluorescence Spectroscopy of Self-trapped Charge-transfer Excitons in Films Dimethylaminobenzylidene 1,3 Indandione (DMABI) *Lithuanian Journal of Physics* 1 1998: pp. 52 – 57.